nature communications

Article

https://doi.org/10.1038/s41467-024-54598-z

Azocarboxamide-enabled enantioselective regiodivergent unsymmetrical 1,2-diaminations

Received: 19 August 2024

Accepted: 14 November 2024

Published online: 26 November 2024

Check for updates

Yun-Dong Fu[1,2,5], Han Zhang[1,5], Bei-Bei Li[1,5], Lihua Huang[1] ✉, Xiao Xiao[3], Min-Can Wang[1], Donghui Wei[1] ✉ & Guang-Jian Mei[1,4] ✉

Enantioenriched unsymmetrical vicinal diamines are important basic structural motifs. While catalytic asymmetric intermolecular 1,2-diamination of carbon–carbon double bonds represents the most straightforward approach for preparing enantioenriched vicinal-diamine-containing heterocycles, these reactions are often limited to the installation of undifferentiated amino functionalities through metal catalysis and/or the use of stoichiometric amounts of oxidants. Here, we report organocatalytic enantioselective unsymmetrical 1,2-diaminations based on the rational design of a bifunctional 1,2-diamination reagent, namely, azocarboxamides (ACAs). Under the catalysis of chiral phosphoric acid, unsymmetrical 1,2-diaminations of ACAs with various electron-rich double bonds readily occur in a regiodivergent manner. Indoles prefer dual hydrogen-bonding mode to give dearomative (4 + 2) products, and 3-vinylindoles and azlactones are inclined to undergo unsymmetrical 1,2-diamination via the (3 + 2) process. DFT calculations are performed to reveal the reaction mechanism and the origin of the regio- and enantioselectivity. Guided by computational design, we are able to reverse the regioselectivity of the dearomative unsymmetrical 1,2-diamination of indoles using Lewis acid catalysis.

Enantioenriched vicinal diamine structural motifs, especially unsymmetrical ones, are frequently identified in pharmaceuticals, agrochemicals, and natural products, and serve as privileged backbones for chiral catalysts or ligands for asymmetric catalysis (Fig. 1A)[1–4]. Accordingly, the development of efficient practical methods for their catalytic asymmetric synthesis has been intensively pursued. The catalytic asymmetric intermolecular 1,2-diamination of readily available carbon–carbon double bonds constitutes the most conceptually straightforward approach for preparing enantioenriched vicinal-diamine-containing compounds (Fig. 1B)[5–10], but alternative methods, including imine cross-coupling, diol diamination, asymmetric hydrogenation, and Mannich-type coupling, have also been described[11–18]. Despite significant achievements made in recent decades[19–27], the established protocols are often limited to the installation of undifferentiated amino functionalities through metal catalysis and/or the use of stoichiometric amounts of oxidants (Fig. 1B, left). From a synthetic perspective, enantioselective unsymmetrical 1,2-diaminations are more attractive because the formed vicinal diamine motifs have two differentiated amino groups, and any of them can be easily orthogonally manipulated in downstream transformations (Fig. 1B, right). However, potential regioselectivity issue pose a daunting challenge. Recently, Glorius and Yang reported elegant racemic examples of regioselective unsymmetrical 1,2-diaminations by using bifunctional nitrogen-radical precursors[28–30]. Inspired by the above work, we have

[1]College of Chemistry, Zhengzhou University, Zhengzhou 450001, China. [2]Henan Academy of Sciences, Institute of Chemistry, Zhengzhou 450046, China. [3]Collaborative Innovation Center of Yangtze River Delta Region Green Pharmaceuticals, Zhejiang University of Technology, Hangzhou, China. [4]Pingyuan Laboratory (Zhengzhou University), Zhengzhou 450001, China. [5]These authors contributed equally: Yun-Dong Fu, Han Zhang, Bei-Bei Li.
✉e-mail: hlh606@zzu.edu.cn; donghuiwei@zzu.edu.cn; meigj@zzu.edu.cn

https://doi.org/10.1038/s41467-024-54598-z

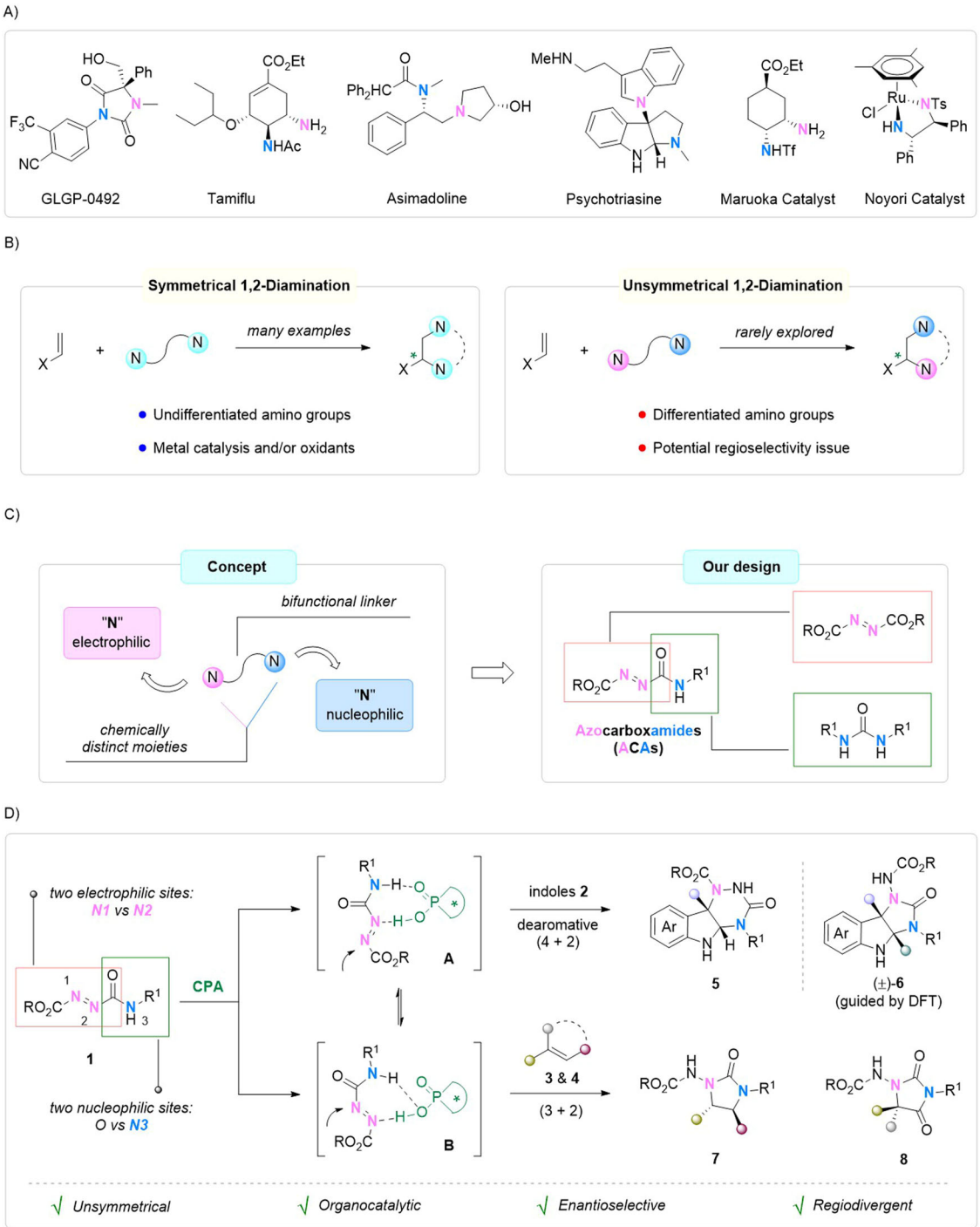

Fig. 1 | Catalytic enantioselective unsymmetrical 1,2-diaminations. A Representative vicinal-diamine-containing compounds. **B** Enantioselective 1,2-diamination of C = C double bonds. **C** Rational design of a bifunctional 1,2-diamination reagent. **D** This work.

decided to develop enantioselective organocatalytic unsymmetrical 1,2-diaminations based on the rational design of bifunctional 1,2-diamination reagents.

It can be rationalized that a successful bifunctional 1,2-diamination reagent should have two chemically distinct "N" moieties for well-defined reactivity and a bifunctional linker for stability (Fig. 1C, left). Therefore, we assumed that the hybrid of azodicarboxylates and urea, namely azocarboxamides (ACAs)[31,32], could be a reasonable choice (Fig. 1C, right). The azo moiety undergoes electrophilic amination[33–38], while the amide moiety undergoes nucleophilic amidation[39]. As a result, regioselective unsymmetrical 1,2-diamination of polarized double bonds is feasible. However, there are two electrophilic sites, N1 and N2, in the azo moiety, and regioselectivity may become a problem. Given the low nucleophilicity of amides (N3), hydroxylamination via carbonyl O-cyclization could be a competing reaction[34]. Here, we report the Chiral phosphoric acid (CPA)-catalyzed regiodivergent enantioselective unsymmetrical 1,2-diaminations of ACAs **1** with various electron-rich double bonds **2**–**4** (Fig. 1D). Under mild conditions, various unsymmetrical vicinal-diamine-containing heterocycles, triazinoindolines **5**, imidazolidinones **7**, and hydantoins **8**, are collectively prepared in good yields with excellent enantioselectivities. Guided by density functional theory (DFT) calculation, we are able to reverse the

https://doi.org/10.1038/s41467-024-54598-z

Table 1 | Reaction optimization for dearomative enantioselective unsymmetrical 1,2-diamination of indoles

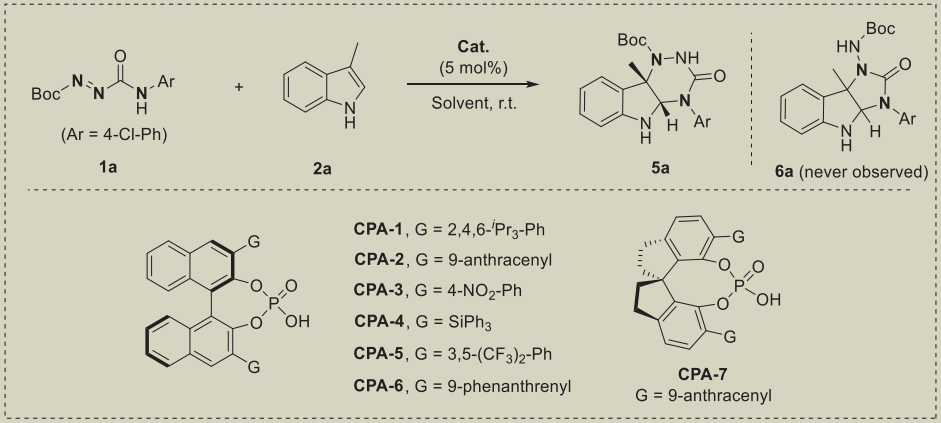

Entry[a]	Cat.	Solvent	Yield (%)[b]	ee (%)[c]
1	**CPA-1**	DCE	33	48
2	**CPA-2**	DCE	64	76
3	**CPA-3**	DCE	25	32
4	**CPA-4**	DCE	47	53
5	**CPA-5**	DCE	60	30
6	**CPA-6**	DCE	73	30
7	**CPA-7**	DCE	62	90
8	**CPA-7**	CH_2Cl_2	78	96
9	**CPA-7**	$CHCl_3$	<5	-
10	**CPA-7**	toluene	63	94
11	**CPA-7**	CH_3CN	22	92

[a] Unless indicated otherwise, **1a** (0.2 mmol), **2a** (0.2 mmol), and **Cat.** (5 mol%) in a specified solvent (1 mL) at room temperature (r.t.) for 24 h, all products dr >20:1.
[b] Isolated yields.
[c] Determined by chiral HPLC analysis.

https://doi.org/10.1038/s41467-024-54598-z

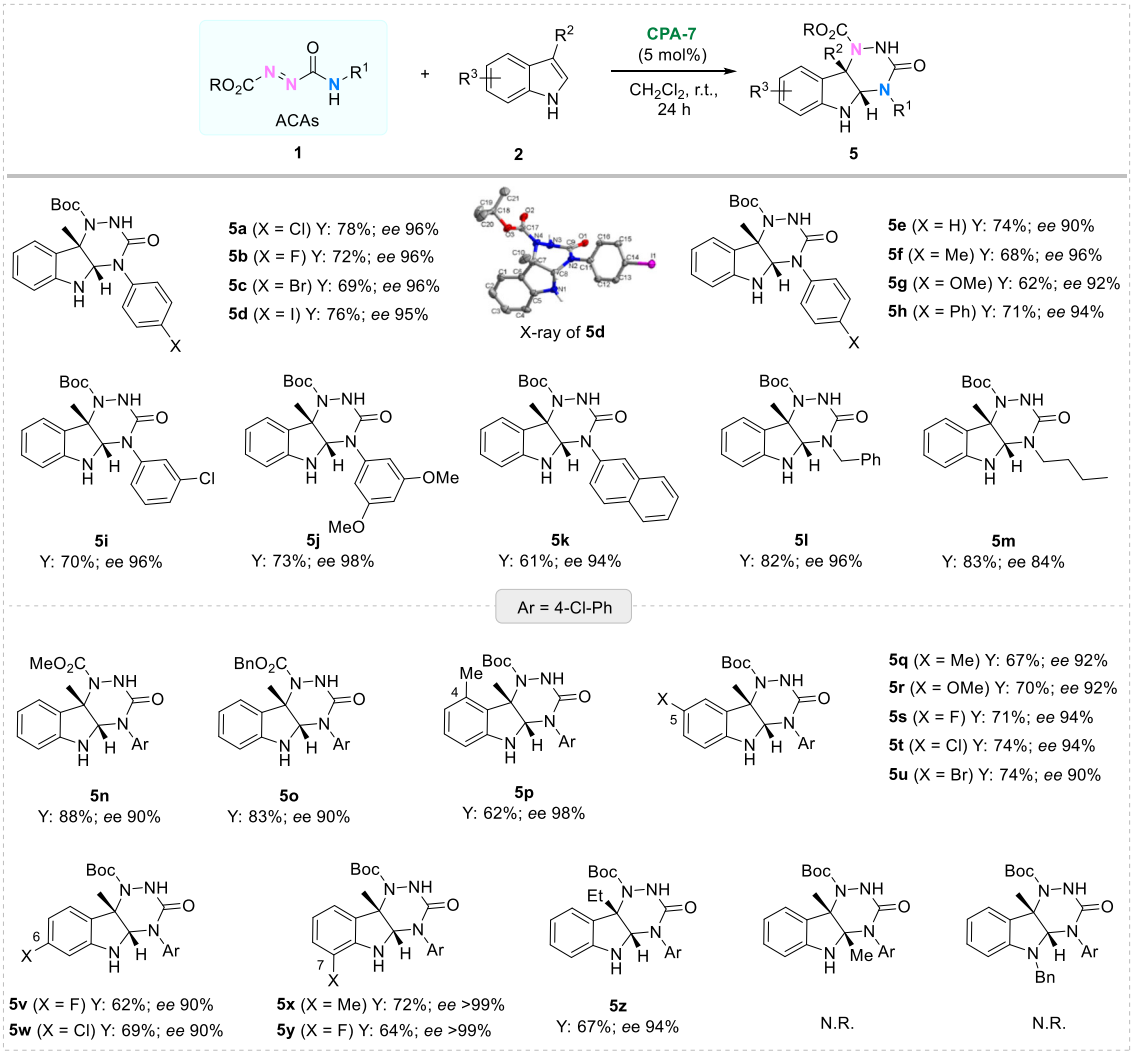

Fig. 2 | Enantioselective unsymmetrical 1,2-diamination of indoles via the dearomative (4 + 2) reaction. Reaction conditions: **1** (0.2 mmol), **2** (0.2 mmol), and **CPA-7** (5 mol%) in CH_2Cl_2 (1 mL) at r.t. for 24 h, all dr > 20:1, isolated yields, *ee* values were determined by chiral stationary HPLC.

regioselectivity of the dearomative unsymmetrical 1,2-diamination of indoles using Lewis acid catalysis.

Results

Reaction optimization

In the initial phase of the investigation, we explored the dearomative unsymmetrical 1,2-diamination between the projected diamination reagent ACA **1a** and 3-methylindole **2a** (Table 1)[40–43]. Under the catalysis of **CPA-1** in dichloroethane (DCE), the dearomative (4 + 2) reaction occurred specifically, providing triazinoindoline **5a** in 33% yield with 48% enantiomeric excess (*ee*). Several commercially available CPAs were then screened, and the results indicated that spiro-CPA **CPA-7** was the best choice (Table 1, entries 1–7). Dichloromethane was identified as the optimal solvent after the study of solvent effect (Table 1, entries 8–11). Finally, the best reaction conditions were those in entry 8, which provided **5a** in 78% yield with 96% *ee*. Notably, the regioselective (3 + 2) product **6a** was never observed during the reaction optimization.

ACA-enabled dearomative (4 + 2) reaction of indoles

With the optimized conditions, we investigated the generality of this CPA-catalyzed dearomative (4 + 2) reaction (Fig. 2). Various ACAs **1** with different substituents were well tolerated. Excellent enantioselectivities were obtained when the *N*-substituents at the amide motif were aromatic groups (**5a**–**5k**). Moreover, an *N*-benzyl-substituted substrate offered product **5 l** in 82% yield with 96% *ee*. However, the enantioselectivity decreased to 84% when an *n*-butyl group was employed (**5 m**). The Boc group appended on the azo motif could be changed to other ester groups, such as -CO_2Me (**5n**) and CO_2Bn (**5o**). Further substrate exploration revealed that all tested indoles **2** with different substituents at varied positions on the benzene ring underwent smooth transformations to produce the desired products **5p**–**5 y** with excellent enantiocontrol. It was feasible to install an ethyl group at the C3 position of the indole to replace the methyl group (**5z**). 2,3-Dimethylindole and *N*-benzylindole were found to be ineffective substrates, likely due to the increased steric hindrance and lack of hydrogen-bonding interactions, respectively. The absolute configuration of **5 d** was determined by X-ray crystallographic analysis, and those of the other products **5** were assigned by analogy.

ACA-enabled enantioselective (3 + 2) reactions

Encouraged by the success of the indole dearomative (4 + 2) reaction, we decided to extend this enantioselective unsymmetrical 1,2-diamination to other nucleophilic double bonds. The vinylogous substrate of indole, 3-vinylindole, was first considered. The experimental results for the reaction between 3-vinylindole **3a** and ACA **1a** with respect to representative CPAs are summarized in the Supplementary Table 2 (page S4). Intriguingly, the regioselectivity was completely reversed, as

https://doi.org/10.1038/s41467-024-54598-z

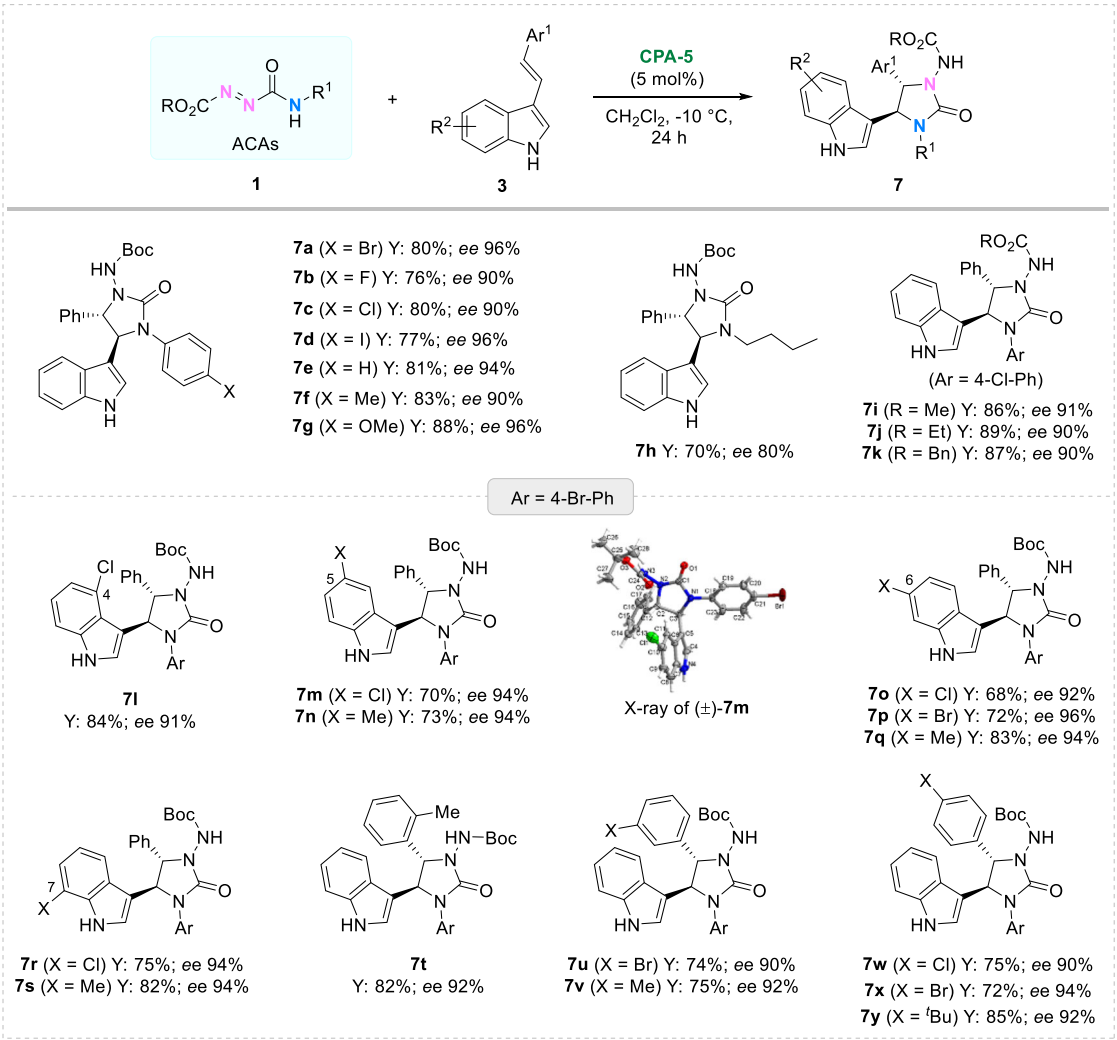

Fig. 3 | Enantioselective unsymmetrical 1,2-diamination of 3-vinylindoles via the (3 + 2) reaction. Reaction conditions: **1** (0.2 mmol), **3** (0.2 mmol), and **CPA-5** (5 mol%) in CH_2Cl_2 (1 mL) at −10 °C for 24 h, all dr > 20:1, isolated yields, *ee* values were determined by chiral stationary HPLC.

only (3 + 2) product **7a** was observed. Under modified reaction conditions with **CPA-5, 7a** was obtained in 80% yield with 96% *ee*. A subsequent probe of the substrate scope afforded an array of highly enantioenriched imidazolidinones in good yields with very good to excellent enantioselectivities (Fig. 3). Installing *para*-substituted phenyl groups on the amide moiety, such as halides (F, Cl, Br, I), hydrogen, methyl, and methoxy groups, had a negligible influence on the reaction outcomes, regardless of the electronic properties (**7a**–**7 g**). Alkyl *n*-butyl group was tolerated but had adverse effects on the enantioselectivity (**7 h**). The variation of the ester groups on the azo motif was feasible and gave consistently good results (**7i**–**7k**). A wide range of 3-vinylindoles **3** were surveyed, affording desired products **7 l**–**7 y** with *ee* values ranging from 90 to 96%, demonstrating the compatibility of 3-vinylindole substrates with the current catalytic system. The relative configuration of **7 m** was determined by X-ray crystallographic and its absolute configuration was determined by circular dichroism spectroscopy analysis (Supplementary Data 1), and those of the other products **7** were assigned by analogy. Subsequently, azlactones **4**, enol surrogates, were tested in this enantioselective organocatalytic unsymmetrical 1,2-diamination. Similar (3 + 2) results were obtained, further demonstrating the chemical divergence of the projected diamination reagent ACAs. The evaluation of the reaction parameters revealed that **CPA-3** was the optimal catalyst (see the Supplementary Table 3, page S5). As depicted in Fig. 4, the reaction exhibited excellent compatibility with substituted ACAs and azlactones, allowing the formation of biologically important hydantoins **8** in good yields with very good to excellent enantioselectivities. Varying the substituents on the amide (**8a**–**8o**) and azo (**8p**–**8r**) groups of the ACAs had no effect on the enantiocontrol. Various ester-containing azlactones were well suited, allowing the formation of highly enantioenriched products **8 s**–**8e′**. However, phenyl-containing azlactone failed to give the corresponding (3 + 2) product because of its low reactivity (see the Supplementary Information, page 105). The absolute configuration of (*ent*)-**8x** was determined by X-ray crystallographic analysis, and those of the other products **8** were assigned by analogy.

Late-stage manipulations

To test the practicality of the developed protocol, late-stage manipulations of these synthesized vicinal-diamine-containing heterocycles were implemented (Fig. 5). Under standard conditions, the synthesis of **5 d** can be carried out on a gram-scale (Fig. 5A). Facile acylation and subsequent Boc-deprotection afforded chiral hydrazine **10**. Oxidation of **10** with *N*-Bromosuccinimide (NBS) gave cyclic azo compound **11**, which served as a chiral reagent in the amination of 2-methylindole. In addition, chiral thiourea **15** was assembled from **7r** via a reaction sequence of Boc-deprotection and thioacylation (Fig. 5B). Finally, several biologically important hydantoin derivatives were readily prepared (Fig. 5C). The *p*-toluenesulfonic acid (*p*-TSA)-triggered

https://doi.org/10.1038/s41467-024-54598-z

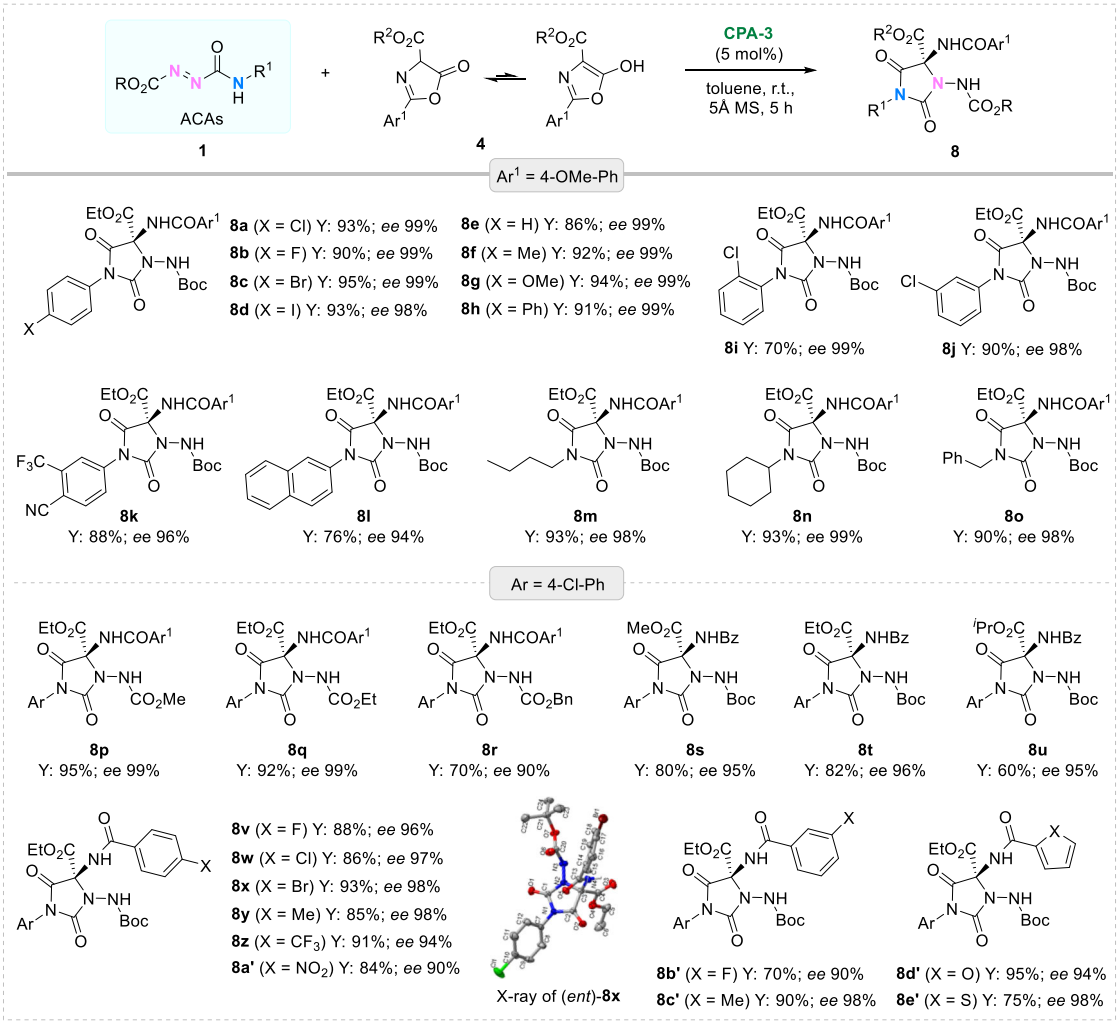

Fig. 4 | Enantioselective unsymmetrical 1,2-diamination of azlactones via the (3 + 2) reaction. Reaction conditions: **1** (0.15 mmol), **4** (0.15 mmol), and **CPA-3** (5 mol%) in toluene (1 mL) at r.t. for 5 h, isolated yields, *ee* values were determined by chiral stationary HPLC.

Boc-deprotection of **8** allowed the formation of *N*-1-amino-hydantoins **16**. Further cyclization under strongly acidic conditions afforded the fused bicyclic compound **17**. Notably, the free *N*-1-amino group can condense with aldehydes to obtain enantioenriched imines **20**, which are chiral analogs of the marked drugs nitrofurantoin and dantrolene[4].

DFT calculations

To discover the general mechanism and origin of the chemo- and enantioselectivity, density functional theory (DFT) calculations were performed using Gaussian16 at the M06−2X[44–46]/6−311 + G(d,p)/IEF-PCM$_{dichloromethane}$[47,48]//M06−2X/6−31 G(d,p)[49,50]/IEF-PCM$_{dichloromethane}$ level, and more computational details were provided in the Supplementary Information page 108-116 and Source Data (Supplementary Data 2). Figure 6 depicts the relative Gibbs free energy profiles of possible (3 + 2) and (4 + 2) cyclization reaction pathways between tert-butyl-2-(phenylcarbamoyl) diazene-1-carboxylate (denoted as **1e**) and indole (denoted as **2a**) catalyzed by **CPA-7**. For the (4 + 2) cyclization, **CPA-7** can firstly combine with **1e** via hydrogen bond interaction (mode A) to form intermediate **I-M0**. Subsequently, **2a** can be complexed with **I-M0** to form intermediate **I-M1R** or **I-M1S**, in which C-N1 bond formation coupled with an intermolecular proton transfer from **CPA-7** to **1e** happens via the diastereomeric transition state **I-TS1R** or **I-TS1S** with an energy barrier of 18.5 or 16.2 kcal/mol, indicating that the *S*-configurational pathway via **I-TS1S** should be the most energetically favorable pathway. Therefore, only *S*-configurational pathway has been discussed in the following part. It should be noted that conformational researches of the stereoselective transition states **I-TS1S** and **I-TS1R** can be found in the SI. The next step is a six-membered ring closure coupled with proton transfer through transition state **I-TS2S** with an energy barrier of 16.8 kcal/mol. The construction of two chiral stereocenters was completed via (4 + 2) cyclization in the intermediate **I-M3S**. Finally, **CPA-7** is dissociation from the (4 + 2) cyclization product and combines with **1e** to form **I-M0** to start next cycle. For the (3 + 2) cyclization reaction pathway, **CPA-7** can combine with **1e** through the hydrogen bond interaction to form intermediate **I-M0'**. intermediates **I-M1R'** and **I-M1S'** can be formed when **2a** is in presence, then C-N2 bond formation coupled with an intermolecular proton transfer with **CPA-7** occurs in mode B via diastereomeric transition state **I-TS1R'** or **I-TS1S'** with Gibbs free energy barrier of 19.0 or 21.7 kcal/mol, which is significantly higher than that of (4 + 2) cyclization pathway and can be excluded safely. As concerned as above, the **CPA-7** catalyzed (4 + 2) cyclization reaction of **1e** and **2a** should be main pathway, and this is consistent with the experimental observation. For the **CPA-7**-catalyzed (3 + 2) and (4 + 2) cyclization of the other substrates including 3-vinylindole **3** and azlactone **4**, we have also investigated the key transition states involved in the first C-N1/N2 bond formation step, and all the calculations are in agreement with the experiments (more computed results can be found in Supplementary Information).

https://doi.org/10.1038/s41467-024-54598-z

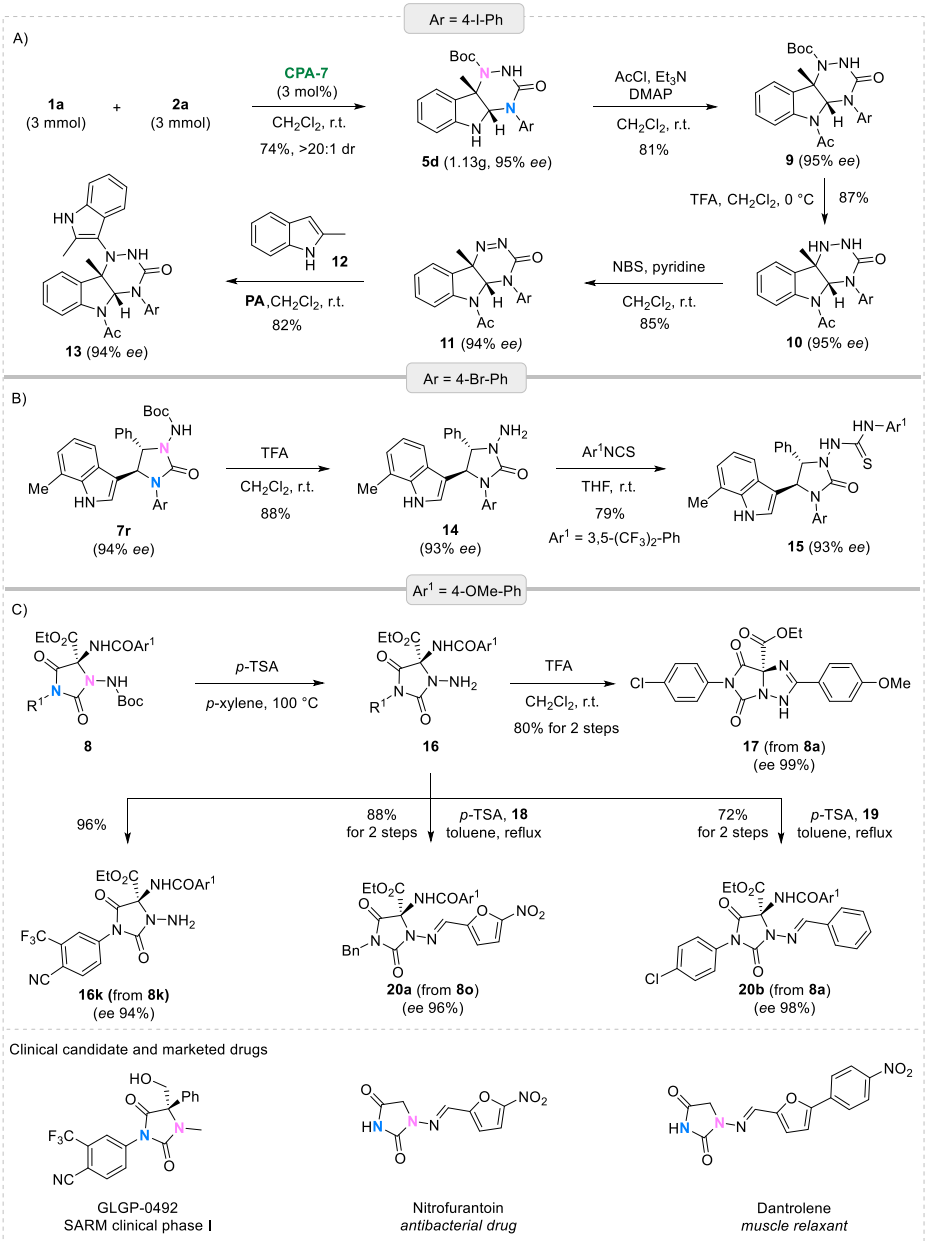

Fig. 5 | Transformations of the prepared vicinal-diamine-containing heterocycles. A Derivatizations of **5 d**. **B** Derivatizations of **7r**. **C** Derivatizations of **8**. Diphenyl phosphate (PA), 5-nitrofuran-2-carbaldehyde (**18**), benzaldehyde (**19**).

To reveal the origin of regioselectivity, we have conducted a local electrophilicity and nucleophilicity analyses on the three studied **CPA**-catalyzed systems[51,52]. The local electrophilic indexes (P_k^+) of the center N1 and N2 atoms of ACAs in the intermediates can be found in Fig. 7. The computational results indicate that the P_k^+ values of the N1 and N2 atoms in the mode A of case study I are 0.66 and 0.55, respectively, indicating the mode A is associated with C-N1 bond formation and the (4 + 2) cyclization pathway. Whereas the P_k^+ values of the N1 and N2 atoms are 0.51 and 0.65 in the mode B, which facilitates the C-N2 bond formation and (3 + 2) cyclization. Compared all the four P_k^+ values, the N1 atom in mode A has the highest activity and should be the actual reactive site in case study I. In the case studies II and III, the N2 atom of ACA in mode B has the highest P_k^+ value, which can be predicted as the most electrophilic site associated with a (3 + 2) cyclization reaction pathway. In summary, the simultaneous interaction of **CPA** and substrate can regulate the electrophilicity of N1 and N2 atoms of ACA to control the regioselectivity.

To disclose the origin of stereoselectivity, we have conducted non-covalent interaction (NCI) and atoms in molecules (AIM) analyses[53,54] on the two stereoselective transition states of the three studied systems. As shown in Fig. 8 and Supplementary Figs. 172 and 175, the two stereoselective transition states within the same system have similar types of weak interactions under the same mode. Taking the **CPA**-catalyzed (4 + 2) cyclization reaction of **1e** and 3-methylindole as an example, weak interactions including two N–H···O (0.99/1.76, 0.58/2.18), three C–H···O (0.37/2.47, 0.25/2.67, 0.22/2.77), three C–H···π (0.34/2.80, 0.23/2.77, 0.20/2.89), two Lp···π (0.24/3.21, 0.24/3.24), one N–H···π (0.27/2.72) and one π···π (0.26/3.20) interactions **I-TS1S** are more and stronger than those (N–H···O (0.82/1.90, 0.65/2.02), three C–H···O (0.47/2.27, 0.31/2.53, 0.31/2.65), two C–H···π (0.28/2.71, 0.33/2.37), two Lp···π (0.25/3.23, 0.23/3.28) and one π···π (0.26/3.18) interactions) in **I-TS1R** (Fig. 8). Noteworthy, the N–H···O weak interaction has the largest Laplacian electron density ($\nabla^2\rho$) in the transition state **I-TS1S**, and plays key role for determining

https://doi.org/10.1038/s41467-024-54598-z

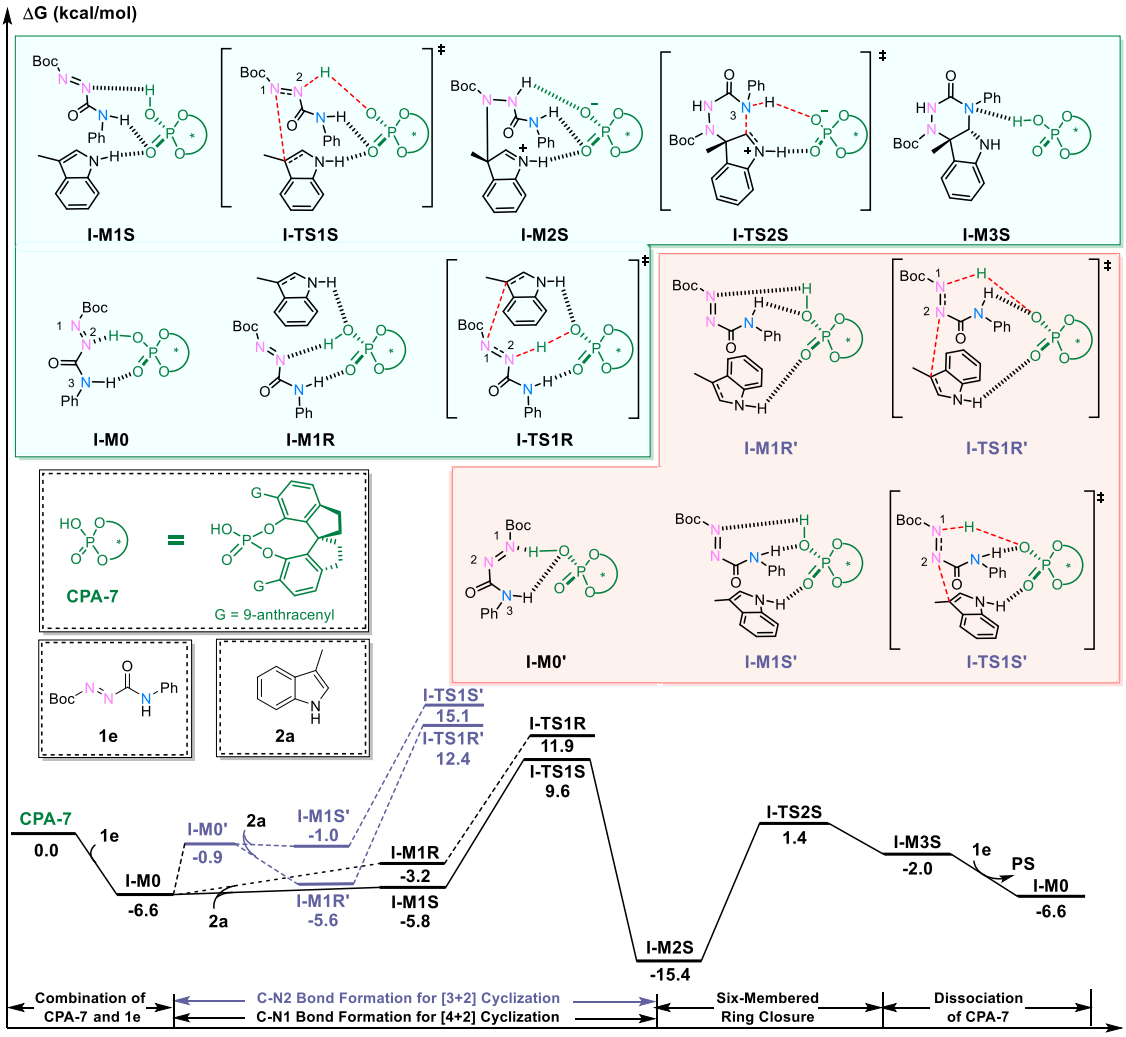

Fig. 6 | The relative Gibbs energy profiles of the different pathways computed at the M06–2X/6–311 + G(d, p)/IEF-PCM$_{dichloromethane}$ //M06–2X/6–31 G(d, p)/ IEF-PCM$_{dichloromethane}$ level of theory. The structures shown in light green and pink color backgrounds are respectively associated with the stationary points involved in **CPA-7** catalyzed (4 + 2) and (3 + 2) cyclizations between **1e** and **2a**.

stereoselectivity. Similarly, the N–H···O weak interactions between substrates and **CPA** are also the strongest in the most favorable transition states in the case studies II and III, and could be responsible for the stability of the most energetically favorable stereoselective transition state (more detailed information and results are available in Supplementary Information).

As concerned as above, the electrophilicity of the nitrogen atoms under different binding modes should be the key factor to control regioselectivity. Considering that Lewis acid (LA) can also strengthen the electrophilicity of substrate, we have further calculated the regioselectivity of dearomative 1,2-diamination reaction of indoles under Lewis acid catalysis. Lewis acids can adsorb the substrate ACA in two similar coordination modes with the modes A and B under CPA catalysis, i.e. mode A' and mode B' (see the Supplementary Table 4, page S114). In both modes, we have calculated the binding energies and analyzed the electrophilicity of ACA in key intermediates using different Lewis acid catalysts. The calculated results indicate that the (3 + 2) cyclization reaction should be the main reaction pathway under Lewis acid catalysis.

ACA-enabled dearomative (3 + 2) reaction of indoles

On the basis of DFT calculations, we decided to use a Lewis acid as the catalyst for the dearomative unsymmetrical 1,2-diamination of indoles with ACAs. As expected, the regioselectivity was completely reversed, resulting in dearomative (3 + 2) products instead of the previous dearomative (4 + 2) product. The screening of the reaction parameters showed that Sc(OTf)$_3$ was found to be the best catalyst, and the addition of PA further improved the yield (see the Supplementary Table 4, page S117). The generality of the reaction was then examined. As displayed in Fig. 9, this dearomative (3 + 2) reaction was applicable to various ACAs and indoles, affording corresponding products **6a–a'** in 63–84% yields. Notably, 2,2-dimethylindole (**6b'**) and *N*-benzylindole (**6c'**) were also well tolerated, indicating that steric hindrance and hydrogen-bonding interaction had no effect on the reaction activity. The relative configuration of (±)-**6a** was determined by X-ray crystallographic analysis, and those of the other products **6** were assigned by analogy. To explore the mechanism, we have conducted DFT calculations of the reaction catalyzed by Sc(OTf)$_3$, and the corresponding Gibbs free energy profiles can be found in the Supplementary Table 5.

Discussions

In conclusion, we have established organocatalytic enantioselective unsymmetrical 1,2-diaminations based on the rational design of bifunctional 1,2-diamination reagent azocarboxamides (ACAs). Under the catalysis of chiral phosphoric acid, the azo moiety undergoes electrophilic amination, while the amide moiety undergoes nucleophilic amidation. Given the two electrophilic sites N1 and N2 in the azo moiety, the unsymmetrical 1,2-diaminations of ACAs with various

https://doi.org/10.1038/s41467-024-54598-z

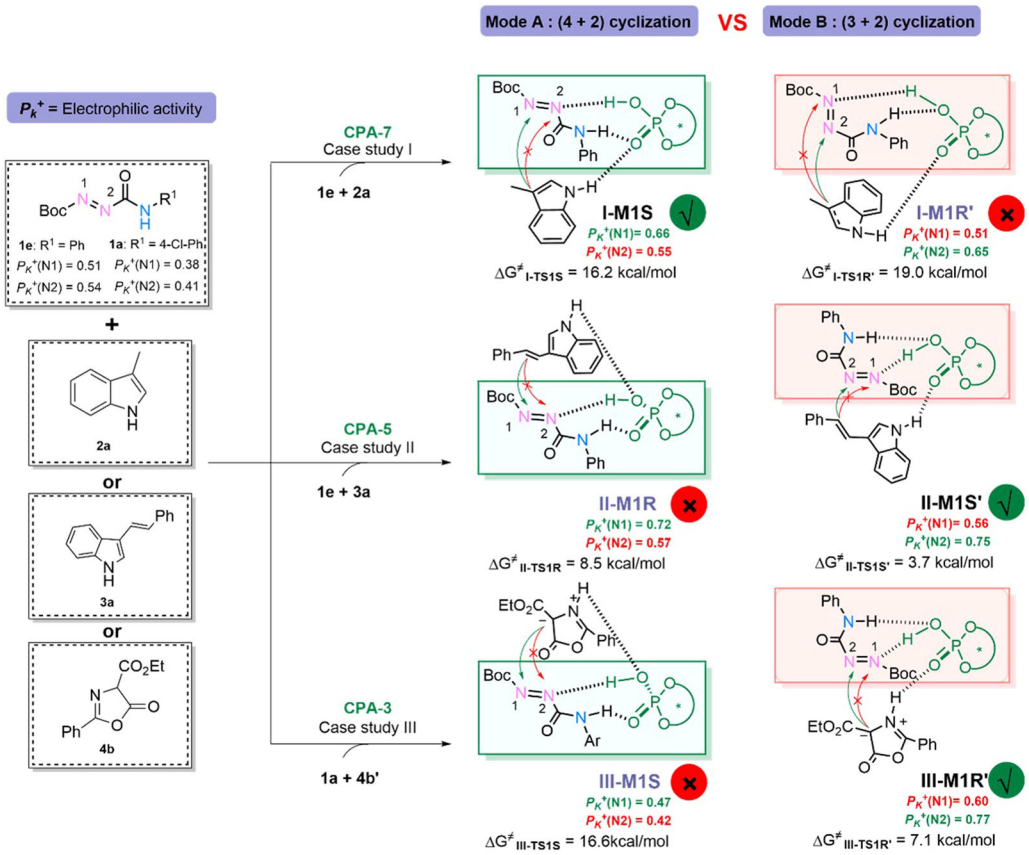

Fig. 7 | The local electrophilicity analyses on the three CPA-catalyzed systems. The local electrophilicity (P_k^+) analyses of **CPA-7** catalyzed reaction of **1e** and **2a**, **CPA-5** catalyzed reaction of **1e** and **3a**, and **CPA-3** catalyzed reaction of **1a** and **4b** were performed, and $\Delta G^{\neq}$ indicates the energy barrier associated with the C-N1/N2 bond formation process.

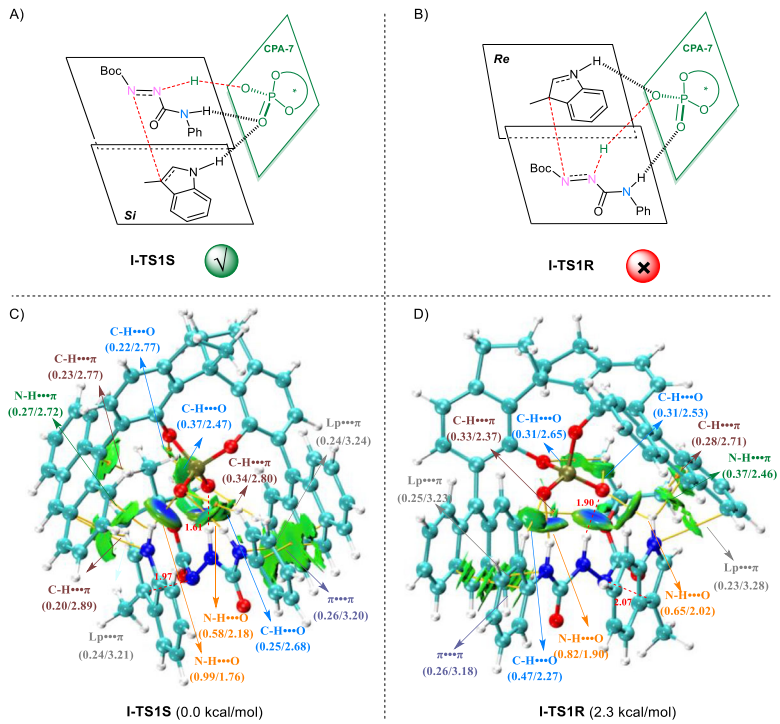

Fig. 8 | NCI and AIM analyses for the transition states I-TS1S and I-TS1R, and the summary of Laplacian electron density ($\nabla^2\rho$ in 10^{-1} a.u.). Optimized structures of transition states **I-TS1S** (**A**) and **I-TS1R** (**B**), NCI and AIM analyses for transition states **I-TS1S** (**C**) and **I-TS1R** (**D**). In the three-dimensional structures, oxygen, nitrogen, carbon, phosphorus, and hydrogen atoms are depicted as red, blue, cyan, brown, and white balls, respectively. Bond critical points (BCPs) along the bond paths were visualized as small orange balls connected by yellow lines.

https://doi.org/10.1038/s41467-024-54598-z

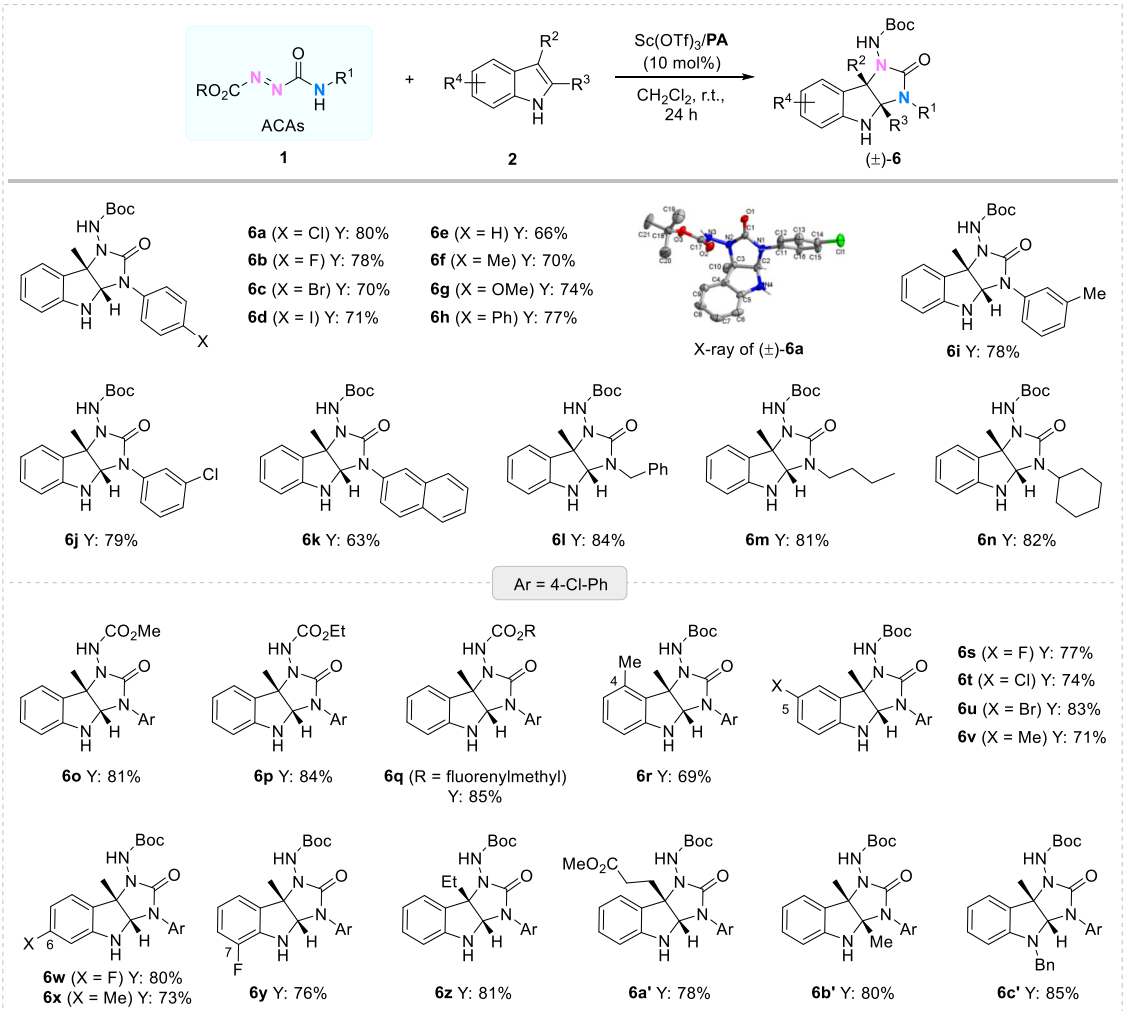

Fig. 9 | Unsymmetrical 1,2-diamination of indoles via the dearomative (3 + 2) reaction. Reaction conditions: **1** (0.2 mmol), **2** (0.2 mmol), and $Sc(OTf)_3$/**PA** (1:1, 10 mol%) in CH_2Cl_2 (1 mL) at r.t. for 24 h, all dr > 20:1, isolated yields. PA = diphenyl phosphate.

electron-rich double bonds could occur in a regiodivergent manner. Indoles preferred dual hydrogen-bonding mode to give dearomative (4 + 2) products, and 3-vinylindoles and azlactones were inclined to undergo unsymmetrical 1,2-diamination via the (3 + 2) process. Under mild conditions, various vicinal-diamine-containing heterocycles, triazinoindolines, imidazolidinones, and hydantoins, were collectively prepared in good yields with good to excellent enantioselectivities. DFT calculations were performed to reveal the reaction mechanism and the origin of the regio- and enantioselectivity. Notably, guided by computational design, we were able to reverse the regioselectivity of the dearomative unsymmetrical 1,2-diamination of indoles using Lewis acid catalysis. In addition to expanding the current library of diamination reagents, the reported ACAs offer facile organocatalytic enantioselective approaches for accessing diverse multi-nitrogen-containing heterocycles. Further applications of ACAs are currently ongoing in our laboratory, and the results will be reported in due course.

Methods

General procedure for the enantioselective synthesis of 5

Indole **2** (0.2 mmol) and **CPA-7** (5 mol%) were dissolved in CH_2Cl_2 (2 mL), a CH_2Cl_2 solution (0.5 mL) of azocarboxamide **1** (0.2 mmol) was then added in 5 minutes. The reaction mixture was stirred at room temperature until the start materials were completely consumed (detected by TLC). The solvent was removed in vacuo and the crude product was separated by flash column chromatography on silica gel (petroleum ether/ethyl acetate = 4:1) to afford **5**.

General procedure for the enantioselective synthesis of 7

3-Vinylindole **3** (0.20 mmol), **CPA-5** (5 mol%) were dissolved in CH_2Cl_2 (1 mL) at −10 °C, a CH_2Cl_2 solution (0.5 mL) of azocarboxamide **1** (0.2 mmol) was then added slowly in 5 minutes. The reaction was stirred at −10 °C until the start materials were completely consumed (detected by TLC). The solvent was removed in vacuo and the crude product was separated by flash column chromatography on silica gel (petroleum ether/ethyl acetate = 4:1) to afford **7**.

General procedure for the enantioselective synthesis of 8

Azocarboxamide **1** (0.15 mmol), azlactone **4** (0.15 mmol) were dissolved in toluene (1 mL), and **CPA-3** (5 mol%), 5 Å MS (50 mg) were added. The reaction was stirred at room temperature until the start materials were completely consumed (detected by TLC). The solvent was removed in vacuo and the crude product was separated by flash column chromatography on silica gel (petroleum ether/ethyl acetate = 4:1 – 2:1) to afford **8**.

General procedure for the synthesis of (±)-6

$Sc(OTf)_3$ (0.02 mmol, 9.8 mg) and diphenyl phosphate (10 mol%) were dissolved in CH_2Cl_2 (2 mL) for 30 min, and indole **2** (0.2 mmol) and azocarboxamide **1** (0.2 mmol) were then added in 5 minutes. The

reaction was stirred at room temperature until the start materials were completely consumed (detected by TLC). The solvent was removed in vacuo and the crude product was separated by flash column chromatography on silica gel (petroleum ether/ethyl acetate 4:1–3:1) to afford (±)–**6**.

Data availability

The authors declare that the data relating to the characterization of products, experimental protocols and the computational studies are available within the article and its Supplementary Information. Data for the crystal structures **5 d, 7 m, 8x** and **6a** reported in this paper are deposited at the Cambridge Crystallographic Data Centre (CCDC) under the deposition numbers CCDC 2369056–2369059. Copies of the data can be obtained free of charge via www.ccdc.cam.ac.uk/data_request/cif. Source data (Supplementary Data 1 and 2) are provided with this paper. Data supporting the findings of this manuscript are also available from the authors upon request.

References

1. Kizirian, J.-C. Chiral Tertiary Diamines in Asymmetric Synthesis. *Chem. Rev.* **108**, 140–205 (2008).
2. Viso, A., Fernández de la Pradilla, R., García, A. & Flores, A. α,β-Diamino Acids: Biological Significance and Synthetic Approaches. *Chem. Rev.* **105**, 3167–3196 (2005).
3. Lucet, D., Le Gall, T. & Mioskowski, C. The Chemistry of Vicinal Diamines. *Angew. Chem. Int. Ed.* **37**, 2580–2627 (1998).
4. Konnert, L., Lamaty, F., Martinez, J. & Colacino, E. Recent Advances in the Synthesis of Hydantoins: The State of the Art of a Valuable Scaffold. *Chem. Rev.* **117**, 13757–13809 (2017).
5. Tao, Z.-L. & Denmark, S. E. Catalytic, Enantioselective Diamination of Alkenes. *Synthesis* **53**, 3951–3962 (2021).
6. Zhang, X. & You, S.-L. Removing the Mask in Catalytic Asymmetric Diamination of Alkenes. *Chem* **3**, 919–921 (2017).
7. Zhu, Y., Cornwall, R. G., Du, H., Zhao, B. & Shi, Y. Catalytic Diamination of Olefins via N–N Bond Activation. *Acc. Chem. Res.* **47**, 3665–3678 (2014).
8. de Figueiredo, R. M. Transition-Metal-Catalyzed Diamination of Olefins. *Angew. Chem. Int. Ed.* **48**, 1190–1193 (2009).
9. Cardona, F. & Goti, A. Metal-catalysed 1,2-diamination reactions. *Nat. Chem.* **1**, 269–275 (2009).
10. Muñiz, K. The development of asymmetric diamination of alkenes with imido-osmium reagents. *N. J. Chem.* **29**, 1371 (2005).
11. Zhou, M. et al. Asymmetric Synthesis of Vicinal Tetrasubstituted Diamines via Reductive Coupling of Ketimines Templated by Chiral Diborons. *Angew. Chem. Int. Ed.* **62**, https://doi.org/10.1002/anie.202300334 (2023).
12. Han, X.-L. et al. Catalytic Asymmetric Imine Cross-Coupling Reaction. *J. Am. Chem. Soc.* **145**, 4400–4407 (2023).
13. Zhou, P., Shao, X. & Malcolmson, S. J. A Diastereodivergent and Enantioselective Approach to syn- and anti-Diamines: Development of 2-Azatrienes for Cu-Catalyzed Reductive Couplings with Imines That Furnish Allylic Amines. *J. Am. Chem. Soc.* **143**, 13999–14008 (2021).
14. Pan, H. J. et al. Catalytic Diastereo- and Enantioconvergent Synthesis of Vicinal Diamines from Diols through Borrowing Hydrogen. *Angew. Chem. Int. Ed.* **60**, 18599–18604 (2021).
15. Zhou, M. et al. Enantioselective Reductive Coupling of Imines Templated by Chiral Diboron. *J. Am. Chem. Soc.* **142**, 10337–10342 (2020).
16. Chen, Y., Pan, Y., He, Y. M. & Fan, Q. H. Consecutive Intermolecular Reductive Amination/Asymmetric Hydrogenation: Facile Access to Sterically Tunable Chiral Vicinal Diamines and N-Heterocyclic Carbenes. *Angew. Chem. Int. Ed.* **58**, 16831–16834 (2019).
17. Shao, X., Li, K. & Malcolmson, S. J. Enantioselective Synthesis of anti-1,2-Diamines by Cu-Catalyzed Reductive Couplings of Azadienes with Aldimines and Ketimines. *J. Am. Chem. Soc.* **140**, 7083–7087 (2018).
18. Chen, J. et al. Carbonyl catalysis enables a biomimetic asymmetric Mannich reaction. *Science* **360**, 1438–1442 (2018).
19. Li, Q., Fang, X., Pan, R., Yao, H. & Lin, A. Palladium-Catalyzed Asymmetric Sequential Hydroamination of 1,3-Enynes: Enantioselective Syntheses of Chiral Imidazolidinones. *J. Am. Chem. Soc.* **144**, 11364–11376 (2022).
20. Lv, D. et al. Iron-Catalyzed Radical Asymmetric Aminoazidation and Diazidation of Styrenes. *Angew. Chem. Int. Ed.* **60**, 12455–12460 (2021).
21. Tao, Z., Gilbert, B. B. & Denmark, S. E. Catalytic, Enantioselective syn-Diamination of Alkenes. *J. Am. Chem. Soc.* **141**, 19161–19170 (2019).
22. Song, J., Zhang, Z.-J., Chen, S.-S., Fan, T. & Gong, L.-Z. Lewis Base/Copper Cooperatively Catalyzed Asymmetric α-Amination of Esters with Diaziridinone. *J. Am. Chem. Soc.* **140**, 3177–3180 (2018).
23. Muñiz, K., Barreiro, L., Romero, R. M. & Martínez, C. Catalytic Asymmetric Diamination of Styrenes. *J. Am. Chem. Soc.* **139**, 4354–4357 (2017).
24. Röben, C., Souto, J. A., González, Y., Lishchynskyi, A. & Muñiz, K. Enantioselective Metal-Free Diamination of Styrenes. *Angew. Chem. Int. Ed.* **50**, 9478–9482 (2011).
25. Du, H., Zhao, B. & Shi, Y. Catalytic Asymmetric Allylic and Homoallylic Diamination of Terminal Olefins via Formal C–H Activation. *J. Am. Chem. Soc.* **130**, 8590–8591 (2008).
26. Du, H., Yuan, W., Zhao, B. & Shi, Y. Catalytic Asymmetric Diamination of Conjugated Dienes and Triene. *J. Am. Chem. Soc.* **129**, 11688–11689 (2007).
27. Gao, H. J. et al. Diversity-Oriented Catalytic Asymmetric Dearomatization of Indoles with o-Quinone Diimides. *Adv. Sci.* **10**, 2305101 (2023).
28. Luo, X.-L. et al. Photocatalytic Unsymmetrical Diamination of Styrenes, Indoles, and Benzofurans Facilitated by Benzotriazolyl and Iminyl Radicals. *Org. Lett.* **26**, 559–564 (2024).
29. Zheng, Y. et al. Regioselective Access to Vicinal Diamines by Metal-Free Photosensitized Amidylimination of Alkenes with Oxime Esters. *Angew. Chem. Int. Ed.* **61**, e202212292 (2022).
30. Tan, G. et al. Energy transfer-enabled unsymmetrical diamination using bifunctional nitrogen-radical precursors. *Nat. Catal.* **5**, 1120–1130 (2022).
31. Liu, B. et al. Chiral gold complex-catalyzed hetero-Diels-Alder reaction of diazenes: highly enantioselective and general for dienes. *J. Am. Chem. Soc.* **135**, 3323–3326 (2013).
32. Lenaršič, R., Kočevar, M. & Polanc, S. ZrCl4-Mediated Regioselective Electrophilic Amination of Activated Arenes with New Alkyl Arylaminocarbonyldiazenecarboxylates: Intermolecular and Intramolecular Reactions. *J. Org. Chem.* **64**, 2558–2563 (1999).
33. Lu, Q.-T., Du, Y.-B., Xu, M.-M., Xie, P.-P. & Cai, Q. Catalytic Asymmetric Aza-Electrophilic Additions of 1,1-Disubstituted Styrenes. *J. Am. Chem. Soc.* https://doi.org/10.1021/jacs.4c04852 (2024).
34. Huang, N., Luo, J., Liao, L. & Zhao, X. Catalytic Enantioselective Aminative Difunctionalization of Alkenes. *J. Am. Chem. Soc.* **146**, 7029–7038 (2024).
35. Yu, S., Bao, H., Zhang, D. & Yang, X. Kinetic resolution of substituted amido[2.2]paracyclophanes via asymmetric electrophilic amination. *Nat. Commun.* **14**, 5239 (2023).
36. Wang, D., Shao, Y. B., Chen, Y., Xue, X. S. & Yang, X. Enantioselective Synthesis of Planar-Chiral Macrocycles through Asymmetric Electrophilic Aromatic Amination. *Angew. Chem. Int. Ed.* **61**, e202201064 (2022).
37. Yang, X. & Toste, F. D. Direct Asymmetric Amination of α-Branched Cyclic Ketones Catalyzed by a Chiral Phosphoric Acid. *J. Am. Chem. Soc.* **137**, 3205–3208 (2015).

38. Wang, S. G., Yin, Q., Zhuo, C. X. & You, S. L. Asymmetric dearomatization of beta-naphthols through an amination reaction catalyzed by a chiral phosphoric acid. *Angew. Chem. Int. Ed.* **54**, 647–650 (2015).
39. Huang, L., Arndt, M., Gooßen, K., Heydt, H. & Gooßen, L. J. Late Transition Metal-Catalyzed Hydroamination and Hydroamidation. *Chem. Rev.* **115**, 2596–2697 (2015).
40. Zhuo, C. X., Zhang, W. & You, S. L. Catalytic asymmetric dearomatization reactions. *Angew. Chem. Int. Ed.* **51**, 12662–12686 (2012).
41. Zheng, C. & You, S.-L. Catalytic Asymmetric Dearomatization by Transition-Metal Catalysis: A Method for Transformations of Aromatic Compounds. *Chem* **1**, 830–857 (2016).
42. Sheng, F.-T., Wang, J.-Y., Tan, W., Zhang, Y.-C. & Shi, F. Progresses in organocatalytic asymmetric dearomatization reactions of indole derivatives. *Org. Chem. Front.* **7**, 3967–3998 (2020).
43. Liu, Y.-Z., Song, H., Zheng, C. & You, S.-L. Cascade asymmetric dearomative cyclization reactions via transition-metal-catalysis. *Nat. Synth.* **1**, 203–216 (2022).
44. Zhao, Y. & Truhlar, D. G. The M06 suite of density functionals for main group thermochemistry, thermochemical kinetics, noncovalent interactions, excited states, and transition elements: two new functionals and systematic testing of four M06-class functionals and 12 other functionals. *Theor. Chem. Acc.* **120**, 215–241 (2008).
45. Zhao, Y. & Truhlar, D. G. Exploring the Limit of Accuracy of the Global Hybrid Meta Density Functional for Main-Group Thermochemistry, Kinetics, and Noncovalent Interactions. *J. Chem. Theory Comput.* **4**, 1849–1868 (2008).
46. Zhao, Y. & Truhlar, D. G. Density Functionals with Broad Applicability in Chemistry. *Acc. Chem. Res.* **41**, 157–167 (2008).
47. Barone, V. & Cossi, M. Quantum Calculation of Molecular Energies and Energy Gradients in Solution by a Conductor Solvent Model. *J. Phys. Chem. A* **102**, 1995–2001 (1998).
48. Mennucci, B. & Tomasi, J. Continuum solvation models: A new approach to the problem of solute's charge distribution and cavity boundaries. *J. Chem. Phys.* **106**, 5151–5158 (1997).
49. Petersson, G. A. et al. A complete basis set model chemistry. I. The total energies of closed-shell atoms and hydrides of the first-row elements. *J. Chem. Phys.* **89**, 2193–2218 (1988).
50. Hariharan, P. C. & Pople, J. A. Accuracy of AH n equilibrium geometries by single determinant molecular orbital theory. *Mol. Phys.* **27**, 209–214 (1974).
51. Domingo, L., Ríos-Gutiérrez, M. & Pérez, P. Applications of the Conceptual Density Functional Theory Indices to Organic Chemistry Reactivity. *Molecules* **21**, 748 (2016).
52. Domingo, L. R., Chamorro, E. & Pérez, P. Understanding the Reactivity of Captodative Ethylenes in Polar Cycloaddition Reactions. A Theoretical Study. *J. Org. Chem.* **73**, 4615–4624 (2008).
53. Bader, R. F. W. A quantum theory of molecular structure and its applications. *Chem. Rev.* **91**, 893–928 (1991).
54. Bader, R. F. W. Atoms in molecules. *Acc. Chem. Res.* **18**, 9–15 (1985).

Acknowledgements

Financial supports from National Natural Science Foundation of China (22371265 and 22208302) and Natural Science Foundation of Henan Province (222300420084) are gratefully acknowledged.

Author contributions

Y.-D.F., B.-B.L., L.H., and X.X. performed and analyzed the experiments. M.-C.W. participated in the early development of the project. H.Z. and D.W. performed the DFT calculations. G.-J.M. conceived and designed the project. G.-J.M. overall supervised the project. All authors prepared this manuscript.

Competing interests

The authors declare no competing interests.

Additional information

Supplementary information The online version contains supplementary material available at https://doi.org/10.1038/s41467-024-54598-z.

Correspondence and requests for materials should be addressed to Lihua Huang, Donghui Wei or Guang-Jian Mei.

Peer review information *Nature Communications* thanks Kelly Bugatti, Peng-Ju Xia, Franca Zanardi and the other, anonymous, reviewers for their contribution to the peer review of this work. A peer review file is available.